Electronic Supplementary Information

Monolithic tandem solar cells comprising electrodeposited $CuInSe_2$ and perovskite solar cells with a nanoparticulate ZnO buffer layer

Yoon Hee Jang,[a] Jang Mi Lee,[ab] Jung Woo Seo,[ac] Inho Kim,[d] and Doh-Kwon Lee*[abc]

[a] Photo-electronic Hybrids Research Center, Korea Institute of Science and Technology (KIST), Seoul 02792, Korea

[b] Division of Nano and Information Technology, KIST School, Korea University of Science and Technology, Seoul 02792, Korea

[c] Green School, Korea University, Seoul 02841, Korea

[d] Center for Electronic Materials, Korea Institute of Science and Technology (KIST), Seoul 02792, Korea

*Corresponding Authors: dklee@kist.re.kr (D.-K. Lee)

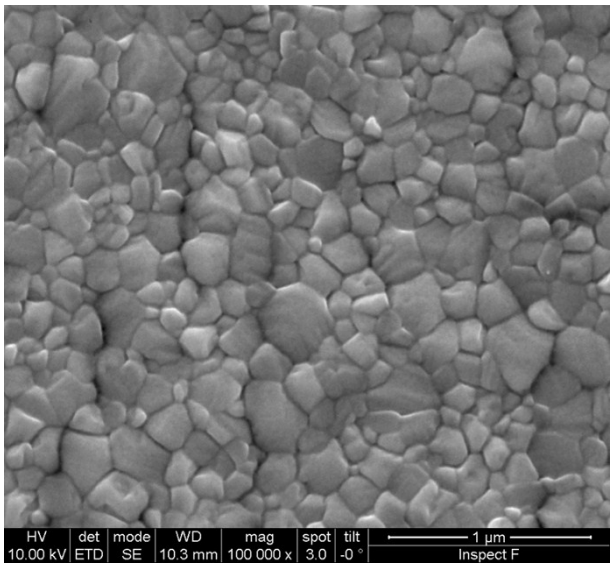

Figure S1. Surface SEM image of a typical $MAPbI_3$ perovskite thin film.

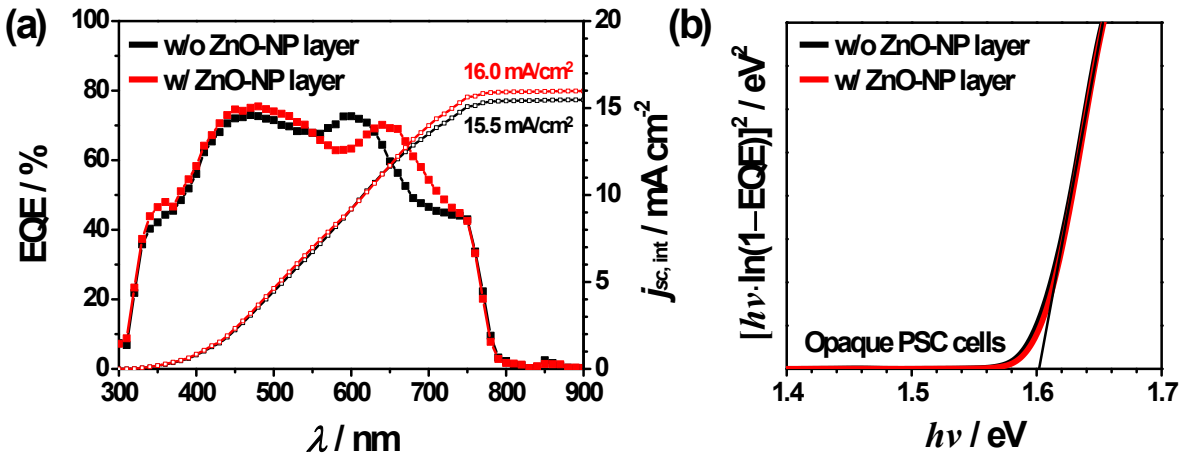

Figure S2. (a) Integrated short-circuit current density ($j_{SC,int}$, right) calculated from EQE curves (left) using the standard AM 1.5G solar spectrum of opaque PSCs with and without a ZnO-NP layer and (b) Plots of $[h\nu \cdot \ln(1 - EQE)]^2$ vs. $h\nu$ near the band edge regime for estimating band gap energies of the PSCs with and without a ZnO-NP layer.

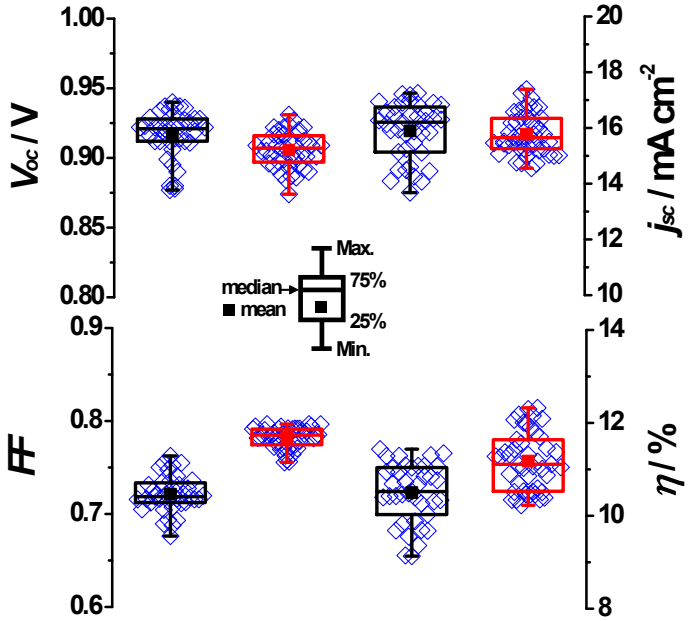

Figure S3. Statistics of photovoltaic parameters of opaque PSCs with (in red) and without (in black) a ZnO-NP layer.

Table S1. Numerical values for the statistics of PV parameters represented in **Figure S3** for opaque PSCs without and with a ZnO-NP layer.

	V_{OC} (V)	j_{SC} (mA cm^{-2})	*FF*	η (%)
Without ZnO	0.92 ± 0.02	15.9 ± 1.0	0.72 ± 0.02	10.5 ± 0.6
With ZnO	0.91 ± 0.02	15.8 ± 0.7	0.78 ± 0.01	11.2 ± 0.6

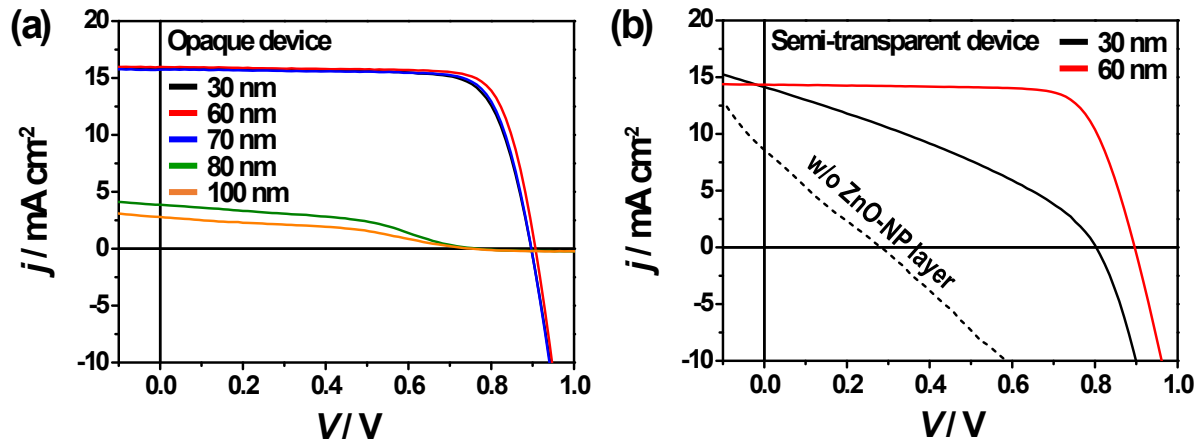

Figure S4. *j*–*V* characteristics of (a) opaque and (b) semi-transparent perovskite solar cells with ZnO-NP layers of various thicknesses. Note that a dotted-line in (b) represents the *j*-*V* curve of a semi-transparent device without a ZnO-NP layer.

Voc (V)	*jsc* (mA cm^{-2})	*FF*	*η* (%)
0.90 ± 0.02	14.3 ± 0.8	0.72 ± 0.05	9.3 ± 0.95

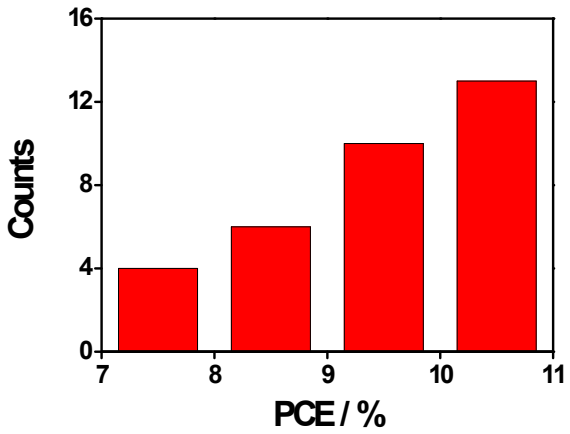

Figure S5. Statistic representation of photovoltaic parameters of 32 semi-transparent PSCs.

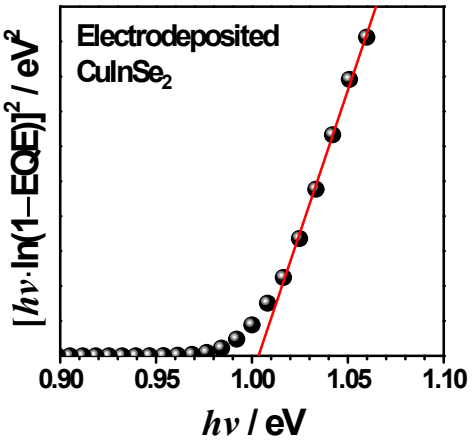

Figure S6. Bandgap estimation of an electrodeposited $CuInSe_2$ solar cell from a plots of $[h\nu \cdot \ln(1 - \mathrm{EQE})]^2$ vs. $h\nu$.

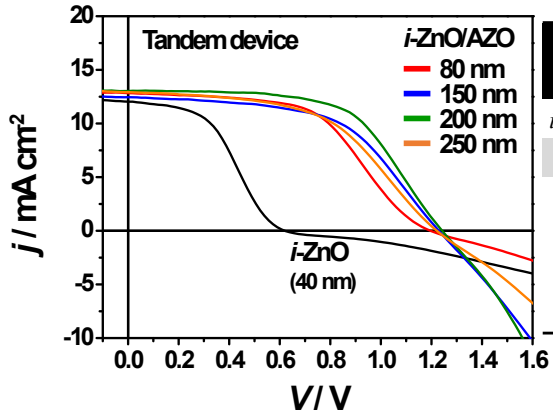

	Voc (V)	*jsc* (mA cm^{-2})	*FF*	η (%)
i-ZnO (40 nm)	0.64 ± 0.02	10.7 ± 1.1	0.41 ± 2.2	2.8 ± 0.4
i-ZnO/AZO Recombination Layer				
80 nm	1.17 ± 0.07	13.1 ± 0.4	0.51 ± 3.7	7.9 ± 1.2
150 nm	1.22 ± 0.01	12.8 ± 0.4	0.55 ± 0.4	8.6 ± 0.2
200 nm	1.24 ± 0.002	12.7 ± 0.2	0.59 ± 0.9	9.2 ± 0.3
250 nm	1.19 ± 0.02	12.6 ± 0.3	0.50 ± 1.3	7.5 ± 0.5

Figure S7. *j*−*V* characteristics of monolithic $CuInSe_2$ (CISe)/perovskite tandem devices as a function of total thickness of the *i*-ZnO/AZO recombination layer and corresponding photovoltaic parameters.

Voc (V)	*jsc* (mA cm^{-2})	*FF*	η (%)
1.25 ± 0.07	13.6 ± 0.9	0.56 ± 0.05	9.5 ± 1.1

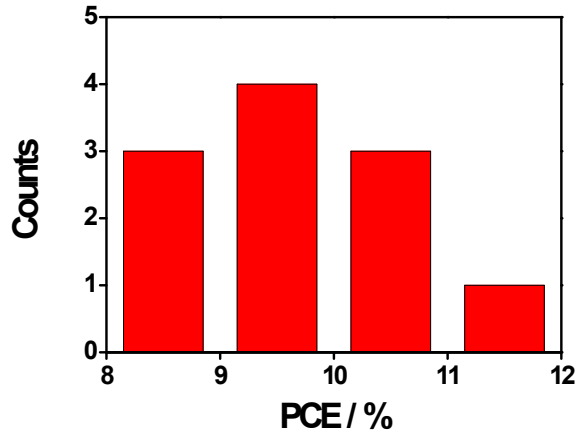

Figure S8. Statistics of photovoltaic parameters of 11 CISe/perovskite tandem devices.

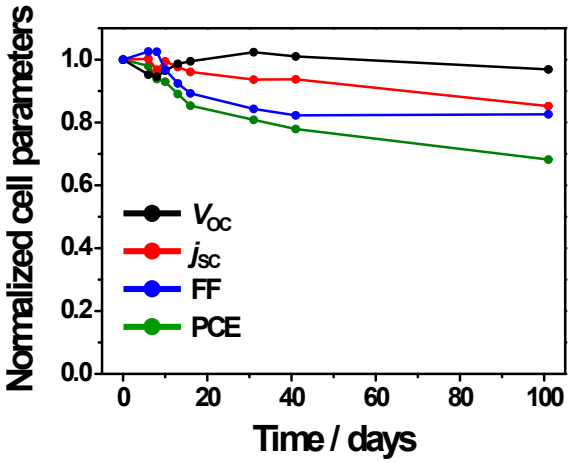

Figure S9. Normalized photovoltaic parameters of a CISe/perovskite tandem device as a function of storing time in a desiccator.